LOOK MUMMY, NO HANDS! THE EFFECT OF TRUNK MOTION ON FORWARD WHEELCHAIR PROPULSION

M.P. van Dijk[1], R.M.A. van der Slikke[1,2], M.A.M. Berger[2], M.J.M. Hoozemans[3], H.E.J. Veeger[1]

[1]Delft University of Technology, Delft, The Netherlands
[2]The Hague University of Applied Sciences, The Hague, The Netherlands
[3]Vrije Universiteit Amsterdam, Amsterdam, The Netherlands

Wheelchair and trunk-mounted IMUs provide a powerful and easy to use method for measuring wheelchair mobility performance. Yet, to develop more specific outcome measures, additional equipment can aid in gaining more insight. A new pushrim hit detection (RhIDE) method was used to investigate forward propulsion measured by frame acceleration in push and recovery phase. Four subjects sprinted at different intensities, while wheelchair velocity, acceleration, trunk movement and push phases were measured. Results show that 25-30% of the total forward propulsion per push (61 to 91 N·s) was performed after hand release. This explorative study shows the significance of propulsion due to trunk movement in the recovery phase. Future research with this measurement setup and daily wheelchair users could help unravel the true share of trunk motion in forward propulsion, and its timing.

KEYWORDS: wheelchair sports, propulsion, trunk motion, contact detection application

INTRODUCTION: Of all Paralympic sports, about one third should or can be performed in a manual wheelchair. Like other cyclic sports, monitoring power or work done by the athlete provides valuable insights for coaches, such as objective measures for training load or training status and may support pacing of a race. For this reason, power meters are already widely used in most cycling disciplines. However, existing power meters for wheelchairs (e.g., OptiPush) have limited application in sports practice, due to their heavy weight and fragility. Furthermore, their measurements are restricted to forces exerted on the rims only.
Although the major forward wheelchair propulsion is produced by the hands, upper body movements can generate propulsion by inertia during the recovery phase (i.e., when the hands are not in contact with the pushrim). The determination of this second propulsion period, due to the backward acceleration of the trunk with respect to the wheelchair, was already reported by Vanlandewijck et al. (1994), yet only on treadmill-based experiments. Quantifying the effect of upper body inertia during overground wheelchair propulsion without changing the wheelchair inertial properties was not yet performed.
Recently, IMU-based methods have been developed that accurately determine wheelchair (van der Slikke et al., 2015) and trunk (van Dijk, 2020) dynamics during wheelchair sports. These can be used to determine a simplified (kinematic) state of the wheelchair-athlete combination over time. With the use of (1) wheelchair and trunk kinematics and (2) a new ‘pushrim hit detection’ system to monitor hand contact, propulsion forces could be estimated. In this way, the first step towards an IMU-based power meter for wheelchair sports can be taken. The current study investigates the effects of trunk motion on forward wheelchair propulsion by quantifying the magnitude and duration of forward wheelchair propulsion during the recovery phase in overground wheelchair sprints.

METHODS: Four able-bodied participants (age 24 $\pm$ 2.6 years, height 1.79 $\pm$ 0.18 m, weight 68.9 $\pm$ 15.3 kg) without wheelchair experience performed a set of straight-line sprints at different intensities with a custom-made Rim Hit Detection (RhIDE) system at one pushrim and NGIMU inertial sensors (xio-technologies) attached to the wheelchair (wheel axis and frame) and their trunk (sternum). All measurements were performed in a sports wheelchair with a rear wheel diameter of 0.62 m and a weight of 11.8 kg with measurement equipment included. Before the session, participants performed a familiarization session in the wheelchair for 15 minutes (Vegter et al., 2014). At the beginning of each exercise, participants were instructed to keep a static posture (and static wheelchair) for at least five seconds. Following this, they performed four sprints in each condition indicated by the instructions 'normal intensity' (condition 1), 'high intensity' (condition 2), 'maximal intensity' (condition 3). The intensities were subjectively ascertained by the participants themselves. After the sprints, deceleration tests were performed in which the participant coasts down from an initial velocity while maintaining a static posture in upright position and in two different inclined trunk angles.

Instrumentation: The NGIMUs provided linear acceleration, gyroscope and magnetometer data (100Hz), used to calculate wheelchair velocity, acceleration and trunk motion. NGIMU analogue input channels of the wheel-mounted sensor were used to apply the RhIDE system. The RhIDE method uses two strips of conductive (woven nickel-copper alloy) tape, placed closely parallel to each other along the perimeter of the pushrim. A voltage of 3.5V was applied to one of the strips to measure short circuit of the system due to hand contact. By detecting contact between user and pushrim, the RhIDE system adds valuable information, while it is hardly noticed by the wheelchair athlete. Since the system doesn't add mass and is automatically synchronized to the IMU data, it is very useful. The RhIDE system was validated for temporal accuracy based on a visual video footage-based inspection. Comparison of pushrim connection times revealed an average underestimation of contact time of 0.03 ± 0.08s.

Data analysis: The gyroscope signal of the wheel IMU was used to obtain wheelchair velocity following van der Slikke et al. (2015). Trunk angle was obtained using a machine learning-based extended Madgwick (MW) filter as described by van Dijk et al. (2020). In this filter, a machine learning model is applied to determine, at each instance in time, whether a low (0.02) or a high (0.96) gain factor is most beneficial based on the raw IMU data. The predicted gain factors and raw IMU data are then entered in the MW filter (Madgwick et al., 2011). Trunk angle was defined as the flexion-extension angle with the vertical with trunk flexion regarded positive. Trunk angle and wheelchair velocity were low-pass filtered with a 6 Hz cut-off.
Given the difference in rolling resistance forces between small caster wheels and the main rear wheels, weight distribution determines overall resistance force. Therefore, the instantaneous resistance force, corrected for trunk orientation, was estimated from the coasting tests. Based on the resistance forces that corresponded to the three different trunk angles in the coasting tests, a first-order polynomial was fit describing the relationship between trunk angle and resistance force when the hands were not in contact with the pushrim. When the hands were in contact with the pushrim, the resistance force was assumed to equal resistance force in upright trunk position.
To determine the magnitude and duration of forward propulsion during each recovery phase, the instantaneous propulsion force was calculated based on the measured wheelchair acceleration and mass of the wheelchair-user combination (Eq. 1-2). The recovery phase timing was obtained from the RhIDE data. Following this, the magnitude of forward propulsion during recovery was determined by calculating the forward propulsion impulse during recovery ($Imp_{propulsion,recovery}$). In addition, the magnitude of the forward resultant during recovery was determined ($Imp_{resultant,recovery}$) as this variable is independent on resistance force estimations, which may include some inaccuracies. The duration of forward propulsion (and forward resultant force) was determined by calculating the difference in time between the onset and offset of forward propulsion (or resultant force). See Table 1 for the definitions of all variables. Since all sprints start from standstill, the first push deviates from the other pushes. Therefore, the second to the fifth push of each sprint were included for further analysis. Results were averaged for the four trials and reported for each condition. A two-way within subjects ANOVA analysis with 'condition' and 'push number' as independent variables was performed to identify whether differences between the conditions were significant ($p<0.05$).

$$F_{resultant} = m_{wheelchair + user} * a_{wheelchair} \quad (1)$$
$$F_{propulsion} = F_{resultant} - F_{resistance} \quad (2)$$

RESULTS: The mean velocity per push ranged from 1.69-1.92 m/s in condition 1 (normal intensity), from 2.27-2.41 in condition 2 (high intensity) and from 2.49-2.77 in condition 3 (max.

intensity). The magnitude of forward propulsion during recovery ranged from 18.9 N·s per push in condition 1 to 22.8 N·s in condition 3 (see Table 2). The duration of this propulsion ranged from 0.29s (condition 1) to 0.20s (condition 3). Of the total forward propulsion, 24.8% (condition 3) to 30.9% (condition 1) was produced during recovery. The magnitude of the forward resultant increased significantly between condition 1 and 3 ($F(2)=4.0$, $p<.05$). Mean trunk angle increased from 33° to 41° between condition 1 and 3 ($F(2)=17.9$, $p<.001$). Tukey's HSD post hoc test revealed differences between condition 1 and 2 ($p<.001$), and 1 and 3 ($p<.001$). The angles ranged from 51°-17°, 61°-21° and 63°-23° in conditions 1, 2 and 3.

Table 1: Variables used for analysis and their definitions

Variable	Definition
$v_{wheelchair}$	Wheelchair velocity; mean wheelchair velocity per push.
$Imp_{propulsion,total}$	Total forward propulsion impulse; mean forward propulsion force ($F_{propulsion}$ in Eq. 2) multiplied by the duration of forward propulsion force.
$Imp_{propulsion,recovery}$	Recovery forward propulsion impulse; mean forward propulsion force during recovery multiplied by the duration of forward propulsion force during recovery.
$Imp_{resultant,recovery}$	Recovery forward resultant impulse; mean forward resultant force (Eq. 1) during recovery multiplied by the duration of forward resultant force during recovery.
Δt_{push}	Push duration; time from first hand-contact until next hand-contact.
$\Delta t_{propulsion,total}$	Total forward propulsion duration; duration of forward $F_{propulsion}$ divided by Δt_{push}.
$\Delta t_{propulsion,recovery}$	Recovery forward propulsion duration; duration of forward $F_{propulsion}$ during recovery divided by Δt_{push}.
$\Delta t_{resultant,recovery}$	Recovery forward resultant duration; duration of forward $F_{resultant}$ during recovery divided by Δt_{push}.

Table 2: Results on the three different conditions expressed as mean (standard deviation)

	1 - Normal intensity	2 - High intensity	3 - Maximal intensity
$v_{wheelchair}$ (m/s)	1.82 (.10)	2.32 (.06)	2.58 (.13)
$Imp_{propulsion,total}$ (N·s)	60.7 (6.9)	80.0 (13.0)	91.2 (22.0)
$Imp_{propulsion,recovery}$ (N·s)	18.9 (10.8)	22.2 (14.7)	22.8 (14.5)
$Imp_{resultant,recovery}$ (N·s)	15.5 (9.1)	19.1 (12.9)	20.4 (13.7)
Δt_{push} (s)	1.20 (.15)	1.08 (.24)	0.89 (.25)
$\Delta t_{propulsion,total}$ (%)	52.7 (1.3)	54.6 (4.7)	56.5 (5.6)
$\Delta t_{propulsion,recovery}$ (%)	23.4 (6.6)	22.3 (7.3)	20.2 (5.6)
$\Delta t_{resultant,recovery}$ (%)	19.9 (5.7)	20.2 (6.9)	18.7 (6.4)

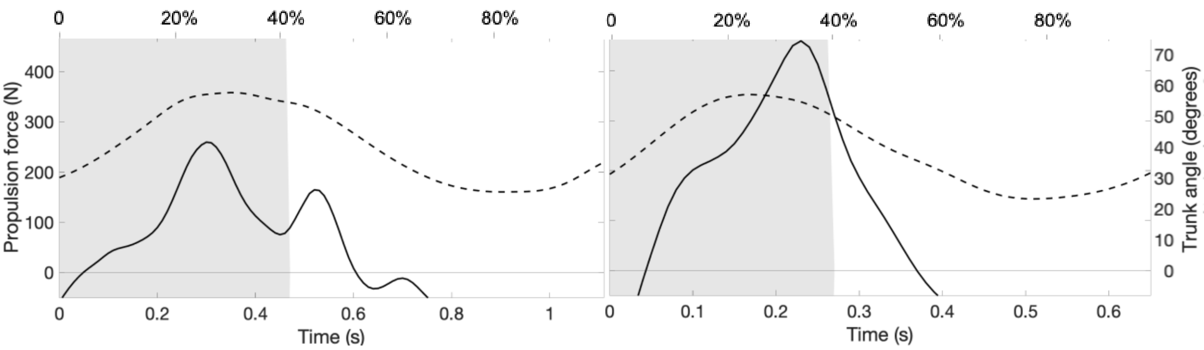

Figure 1: Example of propulsion force (solid line) and trunk angle (dashed line) over time for one push at normal intensity (left) and at maximal intensity (right). The grey surface indicates hand contact.

The left plot in Figure 1 shows a typical example of the propulsion force and trunk angles for one push cycle at normal intensity. The right plot shows these variables at maximal intensity. The propulsion force patterns differ for the two conditions with higher peak forces and less force fluctuations in the maximal condition, while the trunk angle pattern is very similar.

DISCUSSION: The current study investigated the effects of trunk motion on overground forward wheelchair propulsion by quantifying the magnitude and duration of forward wheelchair propulsion forces during the recovery phase. Results revealed that 25-30% of the total propulsion per push was measured after hand release and this trunk-induced propulsion covered 20-23% of the time of the push cycle. The proportion of propulsion generated by trunk motion showed a decreased trend and the mean trunk angle increased for higher intensities. The wheelchair acceleration continues for 0.24 to 0.17s after hand release.

Results show that a considerable part of the wheelchair propulsion takes place after hand release. A similar conclusion has been drawn by Vanlandewijck et al. (1994) who investigated this phenomenon on a treadmill. The current study distinguished impulse that was determined based on positive resultant force (Eq. 1) and impulse based on positive propulsion force (Eq. 2). The results on resultant force reveal that caution should be exercised when interpreting wheelchair acceleration, since up to 20% of this acceleration takes place after hand contact. This implies that, when analyzing manual pushrim force based on wheelchair kinematics only, an overestimation of force duration and an underestimation of force magnitude will likely occur. Although propulsion impulse by the hands was on average larger at high intensities, the trunk-based propulsion impulse remained similar among conditions. This may be explained by the horizontal displacement of the trunk's center of mass (COM) per push, which seem very similar among all conditions. Since both mean trunk angle range and mean trunk angle were larger for high intensities, the horizontal displacement of the trunk's COM per push remained similar. (Note that the horizontal displacement of the trunk COM is not equal to the trunk angle range). With an equal horizontal displacement per push, a 50% higher backward trunk acceleration (thus propulsive force) results in a 50% shorter movement time, resulting in an equal impulse. Since the extent to which wheelchair athletes are able to move and accelerate their trunk differs, the results of this study highlight the effect of trunk motion on propulsion impulse. This insight could be of guidance for future propulsion measurements in athletes with full or reduced trunk mobility. Since a considerable part of the propulsion is generated by the trunk in able-bodied wheelchair users and since unexperienced wheelchair users seem to move their trunk effectively even after a short familiarization period, it might be argued that moving the trunk during wheelchair sprinting is efficient.

This study provided some useful outcomes and proved the concept of trunk motion-based propulsion, albeit a few limitations should be considered. First of all, the sample size was small and included able-bodied individuals. Verification of the results in wheelchair athletes is thus still required. Second, the propulsive forces were not measured directly, but calculated from the resultant force and resistance force. Although, the resistance force is estimated with great care, and assumptions made (about the relation between trunk angle and resistance force) were verified based on the coasting tests, some inaccuracies may still exist. Third, the RhIDE system was located at a single pushrim, while having the system at both pushrims may provide higher accuracy. Since only straight-line sprints were performed in the study, it was assumed that possible left-right differences in hand contact had a negligible effect on the results.

CONCLUSION: The current study investigated the effects of trunk motion on overground forward wheelchair propulsion during the recovery phase. Results demonstrated that 25-30% of the total forward propulsion per push was performed after hand release which took on average 0.20-0.29s. Within this research, trunk motion showed a considerable effect on forward wheelchair propulsion during the recovery phase of a wheelchair sprint. Therefore, caution is advised when estimating pushrim force based on wheelchair kinematics only.

REFERENCES

Madgwick, S.O.H., Harrison, A.J.L., Vaidyanathan, R. (2011). Estimation of IMU and MARG orientation using a gradient descent algorithm. *IEEE International conference on rehabilitation robotics*.

van der Slikke, R.M.A., Berger, M.A.M., Bregman, D.J.J., Lagerberg, A.H., Veeger, H.E.J. (2015). Opportunities for measuring wheelchair kinematics in match settings. *Journal of Biomechanics*, 48(12).

Van Dijk, M.P. (2020) Measuring trunk motion during wheelchair propulsion using wearable inertial sensors (unpublished master's thesis).

Vanlandewijck, Y. C., Spaepen, A. J., Lysens, R.J (1994). Wheelchair propulsion efficiency: movement pattern adaptations to speed changes. *Medicine and Science in sports and exercise*.

Vegter, R.J.K., Lamoth, C.J., de Groot, S. (2014). Inter-Individual Differences in the Initial 80 Minutes of Motor Learning of Handrim Wheelchair Propulsion. *PLOS ONE*, 9(2):10.